Electronic Supplementary Information

Thermo- and photo-modulation of exciplex fluorescence in a 3D spin crossover Hofmann-type coordination polymer

T. Delgado, M. Meneses-Sánchez, L. Piñeiro-López, C. Bartual-Murgui, M. C. Muñoz, J. A. Real.

Experimental Section

Materials

$K[Au(CN)_2]$, $Fe(BF_4)_2 \cdot 7H_2O$ and $Zn(BF_4)_2 \cdot 7H_2O$ were purchased from commercial sources and used as received whereas the synthesis of the bpben ligand was performed as described elsewhere.[1]

Crystal growth

Single crystals of **1Fe@pyr** were grown by slow liquid-liquid diffusion technique using a modified H-vessel with a third tube added due to the limited solubility of the bpben in methanol where the $Fe(BF_4)_2 \cdot 6H_2O$ and $K[Au(CN)_2]$ salts were dissolved. The peripheral tubes (total volume ca. 10 mL) contained $Fe(BF_4)_2 \cdot 6H_2O$ (0.049 mmol, 16.47 mg) and $K[Au(CN)_2]$ (0.098 mmol, 33.38 mg) salts, respectively. The central tube (total volume ca. 10 mL) contained bpben ligand (0.058 mmol, 13.58 mg). Each individual tube was filled with methanol and finally with a saturated solution of pyrene in methanol. Afterwards, the tubes were closed and two weeks later, light-yellow single crystals were formed in the tube which originally contained $Fe(BF_4)_2 \cdot 6H_2O$ salt with relative high yield (ca. 50%). The synthesis of the homologue **1Zn@pyr** was carried out following the same procedure.

EDX analysis (Energy dispersive X-Ray analysis) confirmed the stoichiometric relationship between metallic coordination centers [Fe:Au] and [Zn:Au] = [1:2]. *Elemental Analysis* for **1Fe@pyr**: Calculated for $C_{36}H_{22}Au_2FeN_6$ (988.4) (%): C 43.75; H 2.24; N 8.50. Found (%): C 44.40; H 2.31; N 8.35. *Elemental Analysis* for **1Zn@pyr**: Calculated for $C_{36}H_{22}Au_2ZnN_6$ (997.9) (%): C 43.33; H 2.22; N 8.42. Found (%): C 43.75; H 2.29; N 8.28.

Physical characterization

Single crystal absorption spectroscopy.

Single crystals of **1Fe@pyr** and **1Zn@pyr** were mounted on a copper plate with a previously drilled hole. One crystal was deposited in the middle of the hole and fixed with silver paste to ensure a good thermal

conductivity. The sample was then introduced into a closed cycle cryostat (Janis-Sumimoto SHI-4.5), which operates between 4 and 300 K and is equipped with a programmable temperature controller (Lakeshore Model 331). The cryostat was introduced into a double beam spectrometer (Varian Cary 5000).

Photoluminescence spectroscopy

The excitation and luminescence spectra were recorded on a Fluorolog 3-22 (Horiba Jobin Yvon), equipped with a water-cooled photo multiplier tube (PMT). A calibration function was applied to account for the wavelength-dependent sensitivity of the photomultiplier tube, the wavelength dependent sensitivity of the photomultiplier tube, the throughput of the analyzing monochromator and the power fluctuation of the xenon lamp. For the ambient temperature measurements a quartz capillary was filled with 5 mg of the 1Fe@pyr or **1Zn@pyr** crystals. For the temperature dependence measurements an ensemble of 1Fe@pyr or **1Zn@pyr** crystal are deposited in a cooper plate and fixed with silver paste nanoparticles to ensure a good thermal conductivity. The sample was then introduced into a closed cycle cryostat (Janis-Sumimoto SHI-4.5), which operates between 4 and 300 K and is equipped with a programmable temperature controller (Lakeshore Model 331). The cryostat was introduced in the Fluorolog.

Magnetic and Photomagnetic measurements

The variable temperature magnetic susceptibility measurements were carried out by using microcrystalline samples (15-20 mg) of the **1Fe@pyr**, using a Quantum Design MPMS2 SQUID susceptometer equipped with a 5.5 T magnet, operating at 1 T and at temperatures from 300-1.8 K. Experimental susceptibilities were corrected for diamagnetism of the constituent atoms by the use of Pascal's constants.

Differential Scanning Calorimetry (DSC)

Calorimetric measurements were performed using a differential scanning calorimeter Mettler Toledo DSC 821e. Low temperatures were obtained with an aluminium block attached to the sample holder, refrigerated with a flow of liquid nitrogen and stabilized at a temperature of 110 K. The sample holder was kept in a dry box under a flow of dry nitrogen gas to avoid water condensation. The measurements were carried out using around 20 mg of powdered sample sealed in aluminium pans with a mechanical crimp. Temperature and heat flow calibrations were made with standard samples of indium by using its melting transition (429.6 K, 28.45 J g^{-1}). An overall accuracy of ±0.2 K in temperature and ±2% in the heat capacity is estimated. The uncertainty increases for the determination of the anomalous enthalpy and entropy due to the subtraction of an unknown baseline.

Single-Crystal X-ray Diffraction

Single-crystal X-ray data were collected with an Oxford Diffraction Supernova diffractometer. In all cases, Mo-Kα radiation (λ = 0.71073) was used. Data scaling and empirical or multiscan absorption corrections were performed. The structures were solved by direct methods with SIR2004[2] and refined

by full-matrix least squares techniques on F^2 with SHELXL.[3] Non-hydrogen atoms were refined anisotropically, and hydrogen atoms were placed in calculated positions and refined in idealized geometries (riding model) with fixed isotropic displacement parameters. Relevant crystallographic data, bond lengths and angles for **1Fe@pyr** and **1Zn@pyr** are gathered in Tables S1- S3. CCDC 1847351-1847353 and 1862017 contain the supplementary crystallographic data for this paper. These data can be obtained free of charge from The Cambridge Crystallographic Data Centre.

Table S1. Crystal data of compounds **1Fe@pyr** and **1Zn@pyr**.

***T* (K)**	**Fe 120 K**	**Fe 280 K**	**Zn 120 K**	**Zn 280 K**
Empirical formula	$C_{72}H_{44}N_{12}Au_4Fe_2$		$C_{72}H_{44}N_{12}Au_4Zn_2$	
Mr	1976.76		1995.80	
Crystal system		monoclinic		
Space group	*Cc*	*Cc*	*Cc*	*Cc*
a (Å)	33.2202(13)	33.557(6)	33.219(3)	33.4492(11)
b (Å)	13.2404(5)	13.117(2)	12.9438(10)	13.0989(5)
c (Å)	15.2020(5)	16.174(2)	16.3125(13)	16.2467(6)
β	113.3920(10)	112.407(5)	111.934(3)	112.538(3)
V (Å^3)	6137.0(4)	6581.7(19)	6506.4(9)	6574.8(4)
Z	4			
F(000)	3712		3744	
D_c (mg cm^{-3})	2.139	1.995	2.037	2.016
μ (Mo-K$_\alpha$)(mm^{-1})	10.042	9.364	9.763	9.662
No. of total reflections [$I>2\sigma(I)$]	23132	10829	27866	7442
R [$I>2\sigma(I)$]	0.0438	0.0404	0.0738	0.0679
wR [$I>2\sigma(I)$]	0.0809	0.0716	0.1969	0.0766
S	1.090	1.012	1.054	0.970

References

(1) Culp, J. T.; Madden, C.; Kauffman, K.; Shi, F.; Matranga, C. Inorg Chem. **2013**, 52, 4205-4216.

(2) Burla, M. C.; Caliandro, R.; Camalli, M.; Carrozzini, B.; Cascarano, G. L.; De Caro, L.; Giacovazzo, C.; Polidori, G.; Spagna, R. J. Appl. Cryst. **2005**, ***38***, 381-388 (SIR2004)

(3) Sheldrick, G. M. Acta Crystallogr C Struct Chem. 2015 Jan 1; 71(Pt 1): 3–8. (SHELXL 2015)

Table S2. Fe-N and Zn-N bond lengths (Å) for **1Fe@pyr** and **1Zn@pyr** respectively.

	M = Fe		**M = Zn**	
	120 K	**280 K**	**120 K**	**280 K**
M1-N1	2.015(8)	2.220(10)	2.187(11)	2.19(2)
M1-N2	2.011(7)	2.208(11)	2.159(12)	2.16(2)
M1-N3	1.940(8)	2.163(11)	2.180(15)	2.18(2)
M1-N4	1.937(8)	2.137(11)	2.110(14)	2.10(3)
M1-N5	1.958(8)	2.179(11)	2.172(13)	2.20(3)
M1-N6	1.930(8)	2.140(11)	2.136(13)	2.14(2)
M2-N7	2.009(7)	2.169(10)	2.126(12)	2.14(2)
M2-N8	1.999(7)	2.136(10)	2.156(12)	2.14(2)
M2-N9	1.920(7)	2.109(12)	2.128(15)	2.17(3)
M2-N10	1.934(7)	2.125(11)	2.147(14)	2.18(2)
M2-N11	1.936(7)	2.147(11)	2.133(14)	2.14(2)
M2-N12	1.926(7)	2.104(12)	2.115(14)	2.16(3)
dM-N	1.965/1.954	2.175/2.132	2.157/2.134	2.16/2.16

Table S3. N-Fe-N and N-Zn-N bond angles (°) for **1Fe@pyr** and **1Zn@pyr** respectively.

	M = Fe		**M = Zn**	
	120 K	**280 K**	**120 K**	**280 K**
N1-M1-N2	179.4(4)	178.5(5)	178.9(5)	178.5(12)
N1-M1-N3	92.3(3)	93.6(4)	92.9(5)	91.9(9)
N1-M1-N4	88.3(3)	89.1(4)	88.9(5)	89.8(10)
N1-M1-N5	90.5(3)	89.9(4)	89.6(5)	90.0(9)
N1-M1-N6	88.8(3)	88.5(4)	88.5(5)	88.3(9)
N2-M1-N3	88.0(3)	87.6(4)	88.1(5)	87.3(9)
N2-M1-N4	91.3(3)	89.7(4)	90.1(6)	91.0(10)
N2-M1-N5	90.0(3)	90.9(4)	90.8(5)	91.3(10)
N2-M1-N6	90.7(3)	90.6(4)	91.0(5)	90.3(10)
N3-M1-N4	179.4(4)	177.2(6)	178.2(7)	178.2(12)
N3-M1-N5	91.3(3)	91.4(4)	91.8(5)	91.3(9)
N3-M1-N6	89.0(3)	88.8(5)	87.1(6)	87.1(10)
N4-M1-N5	88.7(3)	88.0(5)	88.5(5)	89.4(12)
N4-M1-N6	90.9(3)	91.9(5)	92.7(6)	92.3(11)
N5-M1-N6	179.3(4)	178.4(5)	177.8(6)	177.6(11)
N7-M2-N8	178.9(3)	179.3(5)	178.6(5)	178.3(10)
N7-M2-N9	89.9(3)	89.5(4)	90.3(5)	89.3(9)
N7-M2-N10	91.7(3)	89.9(4)	89.1(5)	89.7(9)
N7-M2-N11	89.1(3)	92.3(4)	91.9(5)	93.1(9)
N7-M2-N12	89.5(3)	90.0(4)	90.4(6)	88.5(9)
N8-M2-N9	90.5(3)	89.9(4)	90.5(6)	89.3(9)
N8-M2-N10	89.4(3)	90.0(4)	89.7(5)	91.3(9)
N8-M2-N11	90.4(3)	88.3(4)	87.3(6)	88.3(9)
N8-M2-N12	89.4(3)	90.1(4)	90.8(6)	90.4(9)
N9-M2-N10	88.3(3)	87.0(5)	88.6(7)	88.6(11)
N9-M2-N11	178.8(4)	178.1(5)	177.6(6)	177.6(11)
N9-M2-N12	91.1(3)	91.3(4)	90.2(7)	90.5(10)
N10-M2-N11	92.4(3)	92.4(4)	90.4(6)	91.6(8)
N10-M2-N12	178.7(3)	178.3(5)	178.7(8)	178.0(12)
N11-M2-N12	88.2(3)	89.3(5)	90.9(7)	89.4(10)

Figure S1. Coordination centers Fe1 and Fe2.

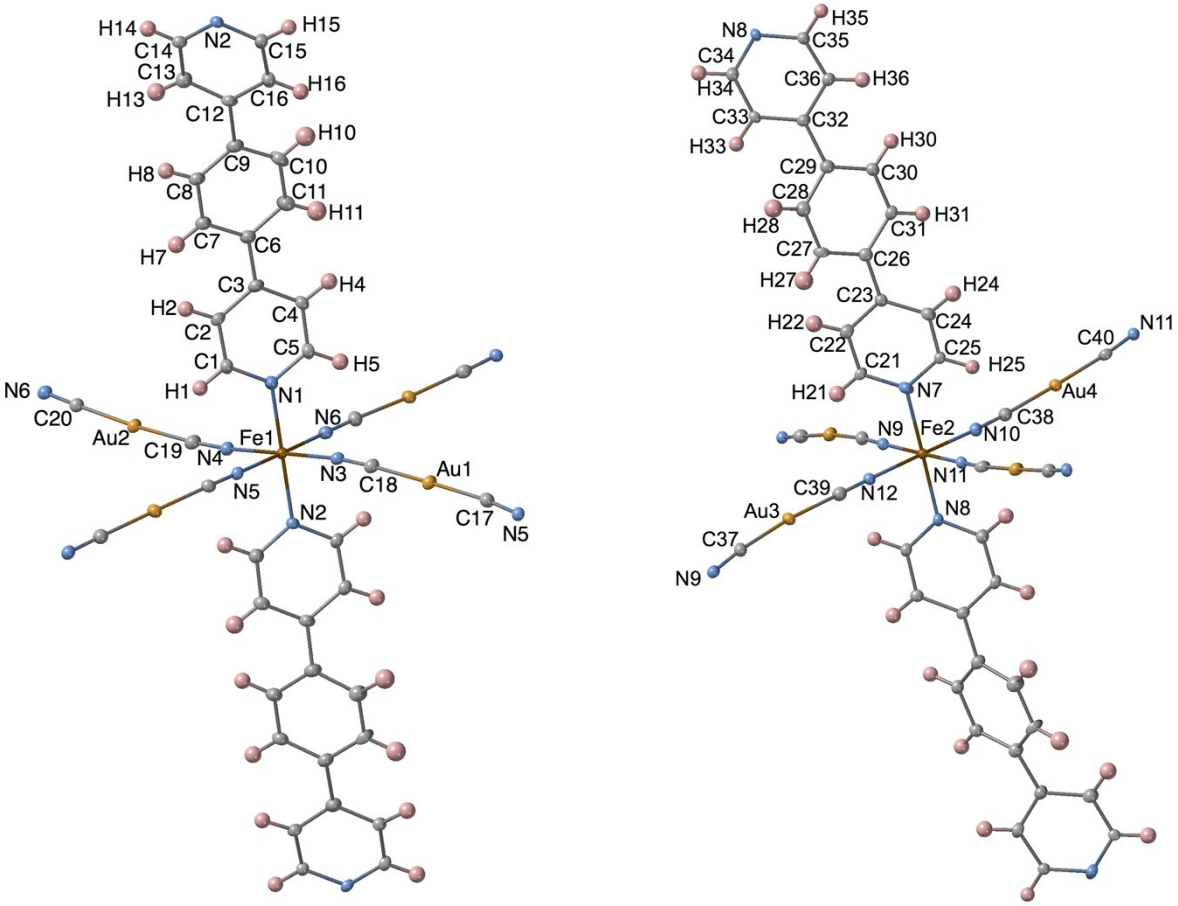

Intermolecular short π-π contacts between pyrene and bpben for **1Fe@pyr**.

C66	C3	3.56886	3.610	C54	C23		3.679
C70	C2	3.57762		C56	C23	3.57	
C60	C6	3.60622					
C70	C3	3.66019					
C68	C11	3.66169					
C70	C4	3.66507	3.558				
C61	C10	3.67164					
C66	C7	3.67272					
C57	C12	3.68590					
C63	C7	3.69025					
C70	C2	3.57762					
C68	C6	3.60622	3.626				
C70	C3	3.66019					
C68	C11	3.66169					
C70	C4	3.66507					
C61	C9	3.50	3.536				
C69	C9	3.53	3.680				
C64	C1	3.35	3.568				

Framework Zn1				Framework Zn2			
Pyrene1	Bpben1	d/Å 120K	d/Å 280K	Pyrene2	Bpben2	d/Å120K	d/Å 280K
C62	C12	3.59	3.63	C53	C33	3.37	3.53
C71	C5	3.44	3.51	C45	C32	3.62	3.61
C59	C7	3.45	3.52	C53	C32	3.54	3.57
C60	C7	3.41	3.42	C53	C29	3.54	3.55
C60	C6	3.57	3.62	C52	C29	3.60	3.61
C62	C9	3.50	3.55	C44	C30	3.68	3.71
C71	C4	3.53	3.57	C52	C30	3.63	3.68
C62	C8	3.35	3.35	C50	C30	3.53	3.54
C65	C2	3.54	3.55	C51	C30	3.54	3.53
C66	C6	3.55	3.57	C51	C31	3.40	3.46
C62	C9	3.50	3.55	C56	C31	3.52	3.57
C58	C8	-	3.63	C56	C26	3.58	3.64
C63	C2	3.69	-	C56	C23	3.64	3.66
C65	C4	3.66	-	C50	C31	3.64	3.68
C65	C3	3.48	3.50				
C60	C8	3.67	3.63				
C66	C3	3.57	3.61				
C64	C2	3.38	3.43				
C61	C8	3.44	3.50				
C57	C8	3.49	3.43				
C70	C4	3.50	3.52				
C70	C5	3.31	3.31				
C69	C10	3.57	3.58				
C61	C9	3.48	3.54				
C69	C9	3.64	3.58				
C64	C1	3.53	3.63				

Table S4-cont. Intermolecular short π-π contacts between pyrene and bpben for **1Zn@pyr**.

Figure S2. Overlay of a representative fragment of the frameworks and pyrene molecule at 280 K (red) and 120 K (green) for (a) Fe(1), (b) Fe(2), (c) Zn(1) and (d) Zn(2) sites.

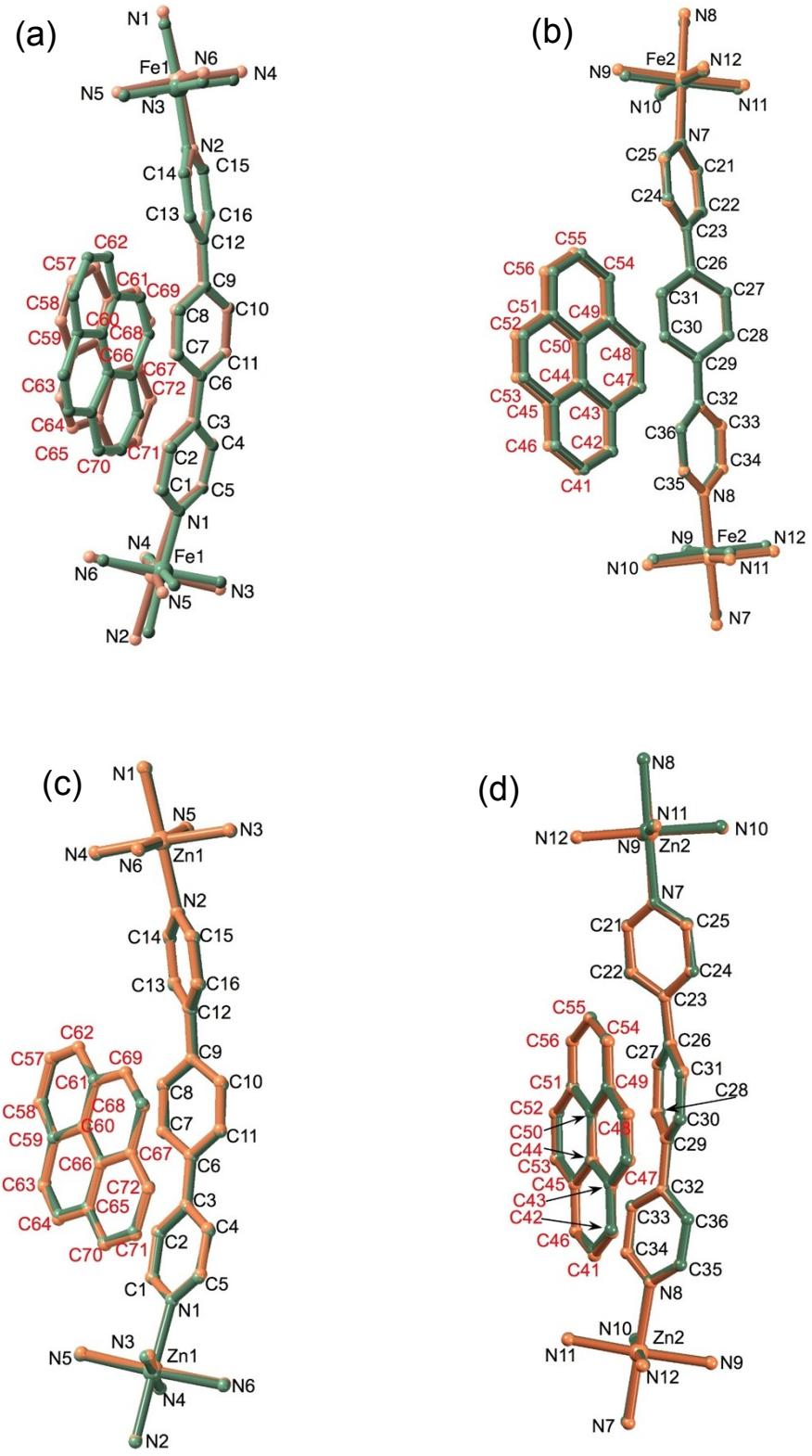
(a)
N1
Fe1
N6
N4
N5
N3
N2
C14
C15
C13
C16
C12
C62
C57
C61
C69
C9
C58
C60
C8
C10
C59
C68
C7
C66
C67
C11
C63
C72
C6
C64
C3
C65
C71
C4
C70
C2
C1
C5
N1
N4
Fe1
N6
N3
N5
N2
(b)
N8
Fe2
N12
N9
N10
N11
N7
C25
C21
C24
C22
C23
C55
C26
C56
C54
C27
C31
C51
C49
C52
C30
C28
C50
C48
C29
C44
C47
C32
C53
C45
C43
C33
C36
C46
C42
C34
C41
C35
N8
N9
Fe2
N12
N10
N11
N7
(c)
N1
N5
N3
N4
N6
Zn1
N2
C14
C15
C13
C16
C12
C62
C9
C57
C69
C61
C10
C8
C68
C58
C60
C7
C59
C67
C11
C66
C6
C63
C72
C3
C65
C64
C4
C70
C71
C2
C1
C5
N1
N3
N5
Zn1
N6
N4
N2
(d)
N8
N11
N12
N10
N9
Zn2
N7
C21
C25
C22
C24
C23
C55
C54
C56
C27
C26
C31
C51
C49
C28
C52
C30
C50
C48
C29
C44
C53
C47
C32
C45
C43
C33
C36
C42
C34
C46
C41
C35
N8
N10
Zn2
N11
N9
N12
N7

Table S5. Geometrical distortion of the bpben ligands: (a) Out of benzene plane distances, D (Å), of the pyridine N atoms coordinated to Fe^{II} (see Scheme I below); (b) Dihedral angles defined between the benzene and pyridine rings. The pyridine rings are denoted by the corresponding N atom.

(a)	Distance D from benzene plane (Å)			
Compound	**1Fe@pyr**		**1Zn@pyr**	
T/K	**120**	**280**	**120**	**280**
N-pyridine atom				
N1	0.545	0.583	0.663	0.713
N2	0.816	0.699	0.619	0.645
N7	0.650	0.424	0.416	0.457
N8	0.556	0.494	0.557	0.685

(b)	Dihedral angle pyridine-benzene planes (°)			
Compound	**1Fe@pyr**		**1Zn@pyr**	
T/K	**120**	**280**	**120**	**280**
Pyridine ring				
N1	11.0	10.9	11.9	13.0
N2	27.7	27.7	28.9	28.3
N7	34.1	34.3	35.5	27.4
N8	30.0	26.1	29.7	32.8

Scheme I. View illustrating the separation of the pyridine N atoms from the average benzene plane as a measure of the bent nature of the bp

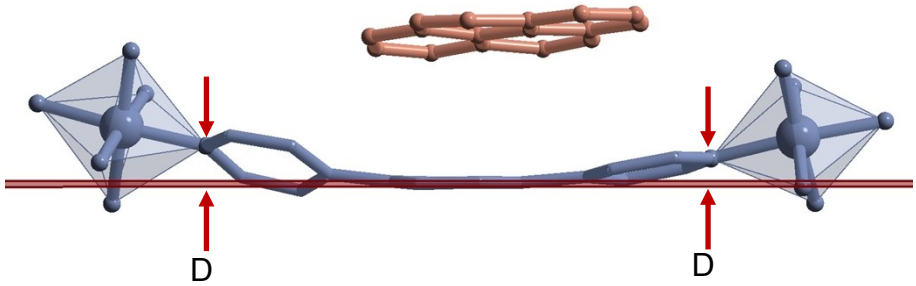

Figure S3. Absorption spectra of a single crystal of **1Fe@pyr** at room temperature and 10 K in the HS (red) and LS (blue) state respectively (left) and temperature variable absorption spectra of **1Fe@pyr** in the cooling mode (right).

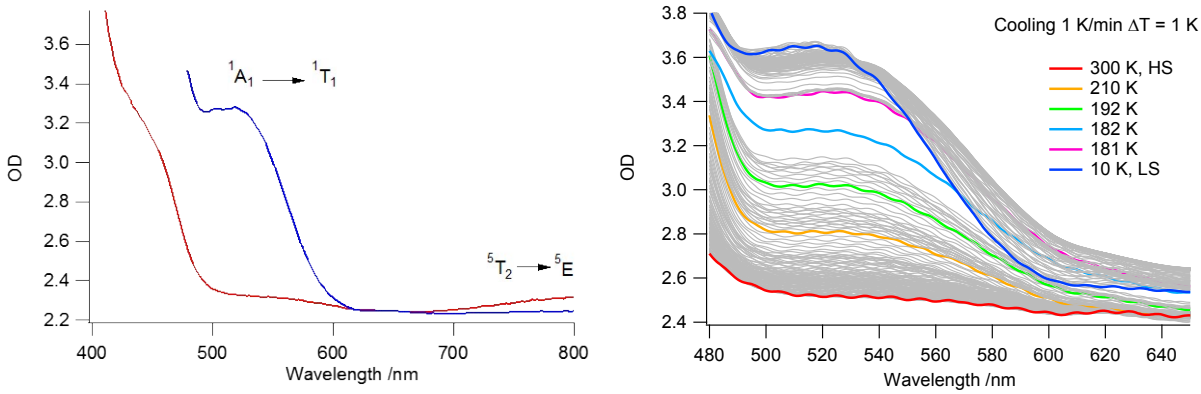

Figure S4. Evolution of the absorption spectra at variable temperature during cooling (top left) and heating (top right) at 5 K/min, and corresponding HS fraction as a function of the temperature established from the optical density difference between 575 and 650 nm (bottom).

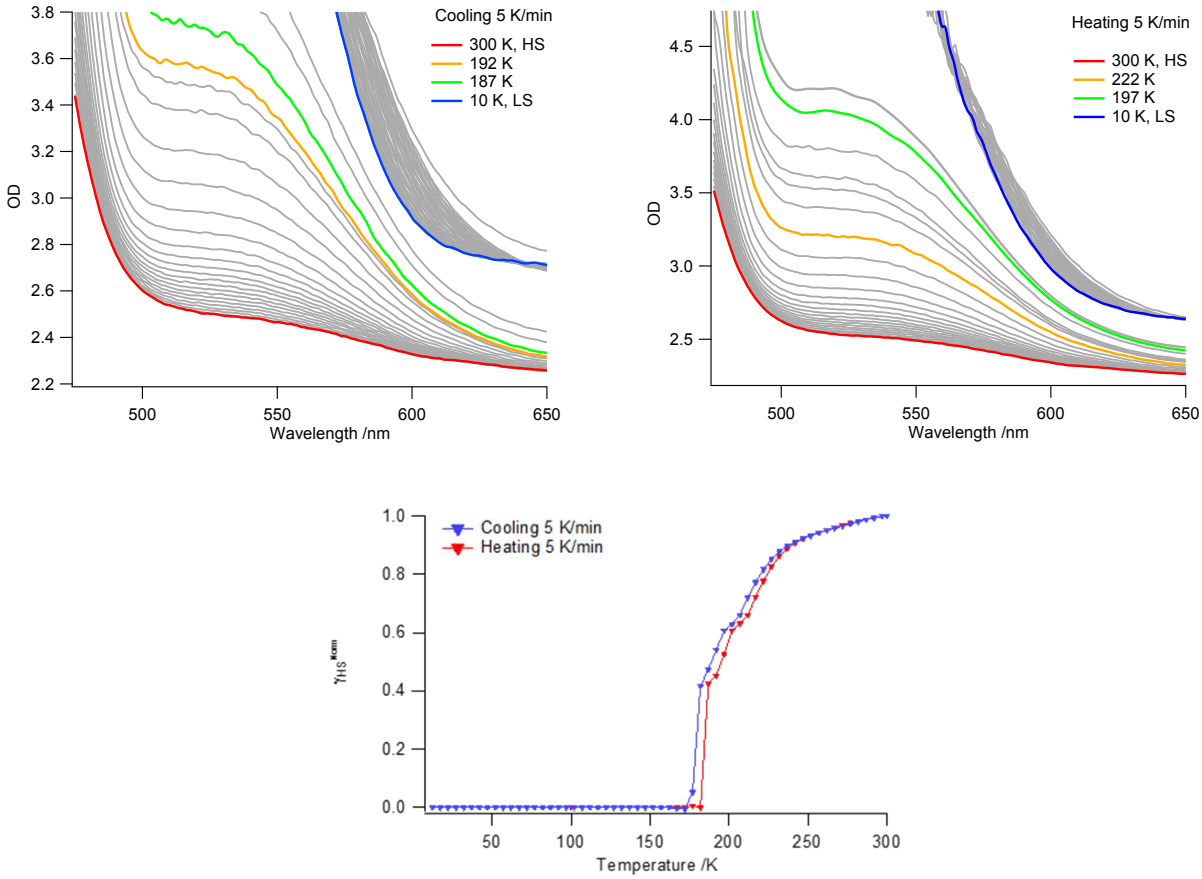

Figure S5. Evolution of the absorption spectra during the HS to LS relaxation after LIESST during heating from 10 to 60 K at 0.3 K/min.

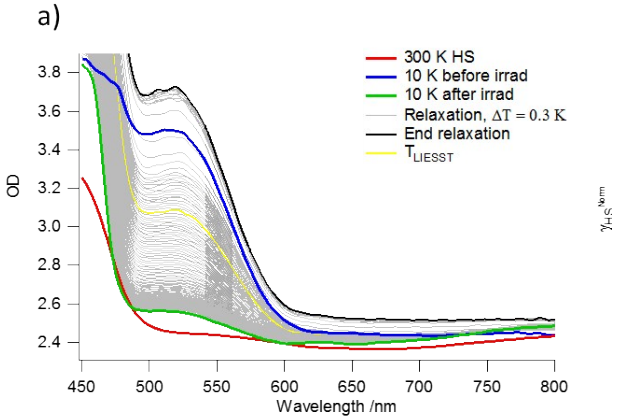

Figure S6. Excitation spectrum of the sample between 250 and 490 nm recorded at 520 nm and corresponding emission spectrum after excitation at 332 nm.

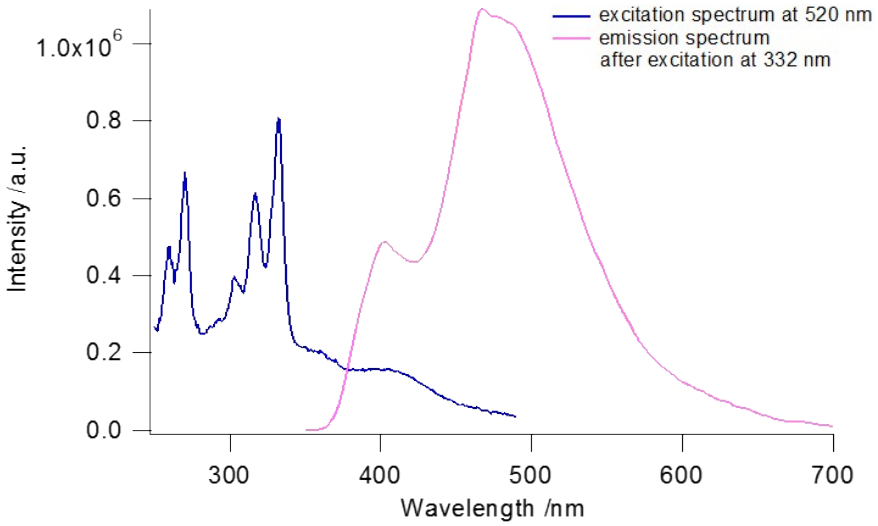

Figure S7. Evolution of the photoluminescence spectra with the temperature during heating at 5 K/min from 10 K to 300 K.